C. R. Geoscience 347 (2015) 227–235

Contents lists available at ScienceDirect

Comptes Rendus Geoscience

www.sciencedirect.com

Hydrology, Environment (Surface Geochemistry)

Late Eocene to present isotopic (Sr–Nd–Pb) and geochemical evolution of sediments from the Lomonosov Ridge, Arctic Ocean: Implications for continental sources and linkage with the North Atlantic Ocean

Ross Stevenson [a,*], André Poirier [a], Alain Véron [b], Jean Carignan [c,1], Claude Hillaire-Marcel [a]

[a] Geotop and Département des sciences de la terre et de l'atmosphère, Université du Québec à Montréal, P.O. Box 8888, Station Centre-Ville, Montréal, Québec H4V 1Y7, Canada
[b] CEREGE, CNRS UMR6635, Université Aix-Marseille-3, Europôle de l'Arbois, BP 80, 13545 Aix-en-Provence cedex 4, France
[c] CRPG-CNRS, 15, rue Notre-Dame-des-Pauvres, 54501 Vandoeuvre-lès-Nancy, France

A R T I C L E I N F O

Article history:
Received 27 November 2014
Accepted after revision 21 February 2015
Available online 21 May 2015

Keywords:
Arctic Ocean
Lomonosov Ridge
Radiogenic isotopes
Basin evolution
Sediment provenance
Anoxic environments

A B S T R A C T

New geochemical and isotopic (Sr, Nd, Pb) data are presented for a composite sedimentary record encompassing the past 50 Ma of history of sedimentation on the Lomonosov Ridge in the Arctic Ocean. The sampled sediments encompass the transition of the Arctic basin from an enclosed anoxic basin to an open and ventilated oxidized ocean basin. The transition from anoxic basin to open ventilated ocean is accompanied by at least three geochemical and isotopic shifts and an increase in elements (e.g., K/Al) controlled by detrital minerals highlighting significant changes in sediment types and sources. The isotopic compositions of the sediments prior to ventilation are more variable but indicate a predominance of older crustal contributions consistent with sources from the Canadian Shield. Following ventilation, the isotopic compositions are more stable and indicate an increased contribution from younger material consistent with Eurasian and Pan-African crustal sources. The waxing and waning of these sources in conjunction with the passage of water through Fram Strait underlines the importance of the exchange of water mass between the Arctic and North Atlantic Oceans.

1. Introduction

In 2004, the Integrated Ocean Drilling Program (IODP) as part of the Arctic Coring Expedition (ACEX) drilled four sites atop the Lomonosov Ridge near 88°N and produced a composite sedimentary record measuring almost 430 m in length and comprising about 55 million years of sedimentary history of the Arctic basin (Backman et al., 2006, 2008). The core preserves the transition of the Arctic basin from an essentially warm anoxic body of water with variable salinity in the Late Cretaceous to the open Arctic Ocean of today (e.g., Pagani et al., 2006; Sluijs et al., 2006, 2008).

Initial studies of the composite sedimentary record revealed that the lower portion of the core consisted of a black shale-like sediment. The character of this sediment, the remnants of fresh water flora (Brinkhuis et al., 2006)

* Corresponding author.
E-mail address: stevenson.ross@uqam.ca (R. Stevenson).
[1] Deceased author.

http://dx.doi.org/10.1016/j.crte.2015.02.008
1631-0713/

and geochemical markers of low oxygen content (März et al., 2011; Poirier and Hillaire-Marcel, 2009, 2011) suggest that during the Paleocene and most of the Eocene, the Arctic basin was a deep anoxic freshwater to slightly saline, lake. In the Late Eocene, the sediments exhibit alternating black and light grey layers referred to as the "Zebra zone" (Backman et al., 2006, 2008). These sediments are interpreted to record the transition from the anoxic Arctic lake stage to a ventilated open ocean (ibid.). This transition interval is characterized by decreasing anoxic conditions and has been interpreted as recording a shallowing of the basin such that the ridge became subaerial for periods of time creating a depositional hiatus and erosion of the sediment on the ridge (Backman et al., 2006, 2008; März et al., 2011). This interpretation has been challenged by Poirier and Hillaire-Marcel (2009, 2011) who propose its deposition under strong current conditions due to the lake drainage/marine submergence following the opening of Fram Strait.

The length of depositional hiatus or even its presence during the transitional interval has thus been the subject of debate. Backman et al. (2006, 2008) interpreted a depositional hiatus of 26 Ma on the basis of dinoflagellate biostratigraphy. März et al. (2011) concluded that their mineralogical and geochemical proxies strongly supported the hiatus as described by Backman et al. (2006). In contrast, Poirier and Hillaire-Marcel (2009, 2011) argued on the basis of:

- Re-Os dating of the anoxic muds on both sides of this sedimentary gap;
- from initial Os isotope ratios of these muds that the Arctic basin did not experience a 26 Ma depositional hiatus.

They suggested that this sedimentary perturbation and marine incursion/ventilation of the Arctic basin lasted about 0.4 Ma at best. The transition from restricted anoxic basin to open Arctic Ocean occurred at 36 Ma. Another hiatus anywhere within the overlying oxic sediments would be invisible to the Re-Os system, because of the low Os (and Re) content of the oxic material, and because of the flatness of the marine osmium evolution curve for that time interval (Poirier and Hillaire-Marcel, 2011).

Radiogenic isotope studies (Sr, Nd, Pb) of sediments from the ACEX core (Fig. 1) encompassing the past 15 million years reflect a mixture of sources from North American and Eurasian sources that show little variation despite repeated glacial periods over the same period (Haley et al., 2008). In contrast, Hillaire-Marcel et al. (2013) demonstrated that the last glaciation was marked by an isotopic (Sr, Nd) excursion during the Youger Dryas that

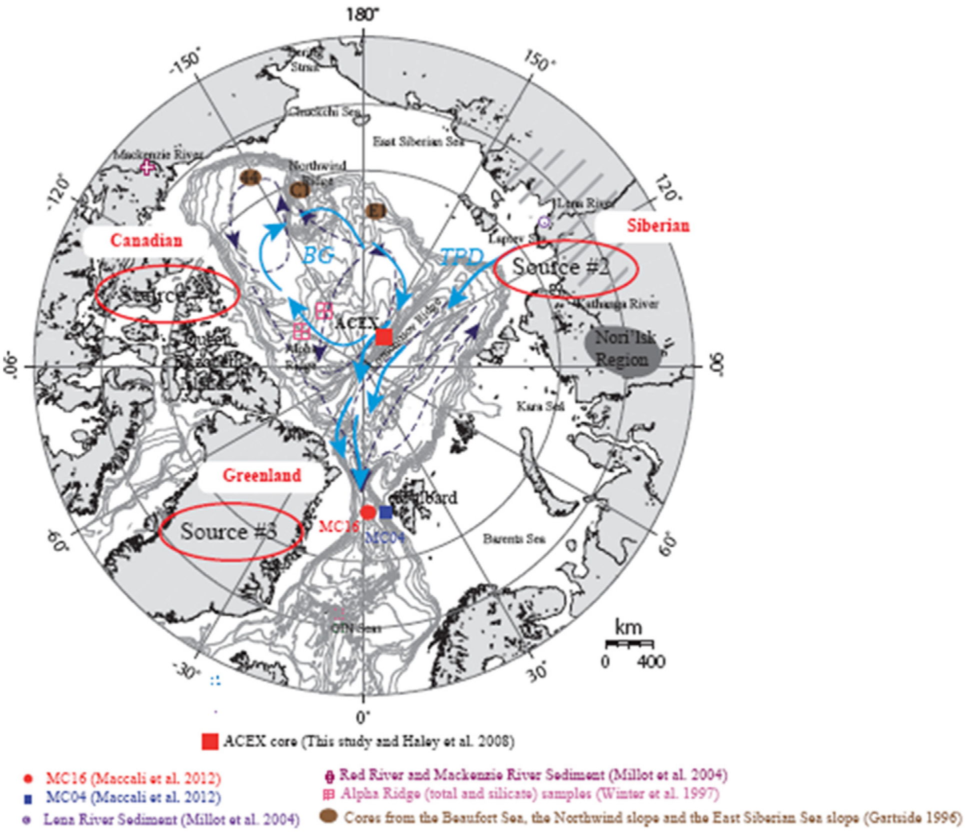

Fig. 1. (Color online.) Map showing location of ACEX core. Also shown are locations of surface sediments and cores discussed in the text as well as the locations of potential sediment sources. BG: Beaufort Gyre; TPD: Trans-Polar Drift.
Modified from Maccali et al., 2012.

correlated with the drainage of Lake Agassiz through the Mackenzie River system. März et al. (2011) described the mineralogical and geochemical changes that accompanied the transition of the Arctic basin from a restricted anoxic basin to an open ventilated ocean. Less well understood is whether these changes reflect wholesale changes in the sediment sources as a result of the opening of the Arctic basin to the open ocean. We present new geochemical (major and trace elements) and isotopic data (Sr, Nd, Pb) for sediments from the composite sedimentary core of the Lomonosov Ridge encompassing the past 50 million years. They provide information on sedimentological and geochemical changes in the Arctic basin from its anoxic to oxic stage. They also shed light on a multi-step transition between these two types of environments.

2. Methods

The sedimentary material was obtained from the IODP repository in Bremen, Germany. The samples were dried in an oven at 45 °C and subsequently ground to powder using an alumina mortar and pestle. The powder was divided into sub-fractions for major and trace element (at CRPG; Nancy, France) and isotopic (Sr, Nd, Pb) analyses.

The powders for isotope analyses were washed and decanted with distilled water and subsequently leached for 3 hours in a solution of 1 M acetic acid and 0.5 M hydroxylamine hydrochloride; a modified version of the leaching procedure described by Gutjahr et al. (2007). This leaching procedure served to remove carbonate (that may be of authigenic origin) and metals bound to authigenic minerals or adhering to detrital phases. The residues were washed in distilled water and dried in preparation for dissolution, chromatography and isotopic analysis. One fraction of the sediment residue was used for Pb–Pb isotope analysis while the remaining fraction was used for Sr isotope and Sm–Nd isotope analysis.

The fraction for Sr and Nd isotopes (0.1 g) was dissolved in a Teflon beaker using a mixture of concentrated hydrofluoric and nitric acids. Details of the Sr and Nd chemistry protocol can be found in Maccali et al. (2013). The Sr and Nd isotopes were analysed on a GV Sector-54 mass spectrometer in dynamic collection mode. The Sr fraction was loaded onto a single Re filament with a Ta oxide activator and the Nd was measured using a double Re filament mode. Repeated measurements of the JNdi-1 Nd standard (Tanaka et al., 2000) yielded a value of $^{143}Nd/^{144}Nd = 0.512106 \pm 7$ (2σ, $n = 37$). Sm and Nd concentrations and $^{147}Sm/^{144}Nd$ ratios have an accuracy of 0.5% that corresponds to an average error on the initial ε_{Nd} value of $\pm$ 0.5 epsilon units. Repeated analysis of the NBS 987 Sr standard yielded a value of $^{87}Sr/^{88}Sr = 0.710263 \pm 17$ (2σ, $n = 7$). Blanks for Sr, Sm and Nd were typically < 150 pg.

For the Pb isotope analyses, about 20 to 40 mg of dried homogenized sediment fractions were dissolved and the Pb separated following the protocol of Maccali et al. (2012). Procedural Pb blanks were always below 40×10^{-12}g. The lead isotope analyses were performed on a Micromass Isoprobe MC–ICP–MS at the GEOTOP laboratories of the Université du Québec à Montréal, using an Aridus desolvating membrane. Data were corrected for instrumental mass bias using thallium doping technique (Belshaw et al., 1998). Long-term reproducibility of the internal standard NBS981standard was better than 0.03% (1σ standard deviation) for all Pb isotopic ratios.

3. Results

3.1. Major and trace element data

Major and trace element data are presented as Supplementary material, Table A1 (data repository). The major element compositions of the sediments fall within three groups that mirror the physical division of the sediments into black muds, zebra muds and grey muds. The black muds are characterized by lower overall totals for the major elements reflecting the high organic matter content of these muds and are depleted in Al, Mg and K compared to the zebra muds and the grey oxic muds. Trace elements that partition into detrital minerals mirror the variations found for the major elements. Elements affected by the reducing conditions in the lower part of the core show large swings in concentrations. März et al. (2011) provide an excellent summary of the different enrichments of the elements in the ACEX composite core. We provide a few examples to demonstrate the concordance of our data suites and to corroborate changes in sedimentary provenance indicated by the radiogenic isotope data below (Fig. 2; see also Fig. 4 below).

3.2. Isotope data (Sr, Nd, Pb)

The isotope data are present in Table 1 and Fig. 3. The Sr isotope ratios of the sediment residues presented on Fig. 3 were not corrected for in-situ decay of ^{87}Rb because the mobility of Rb and Sr in the sediments prohibits the application of the Rb/Sr ratio to correct the measured Sr isotope ratio with any confidence. In any case, the overall age correction would be small as seen with the age-corrected Nd isotope compositions (Table 1). The strontium isotope compositions of the sediments decrease slightly from higher values in the restricted lake phase of the Arctic basin through the transitional period of the zebra muds and flatten out in the ventilated ocean stage.

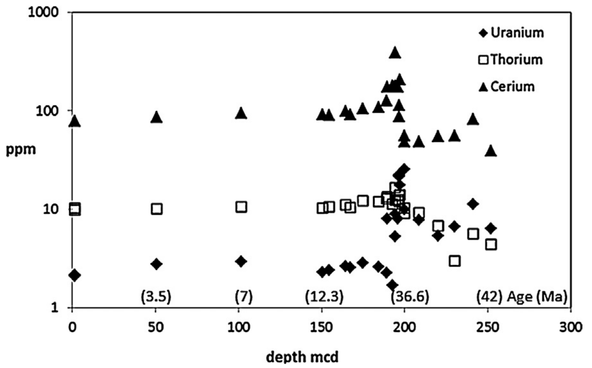

Fig. 2. Changes in the trace element concentrations of uranium, thorium and cerium. Note the strong changes in concentrations of these elements across the transition interval following ventilation and oxidation of the Arctic basin.

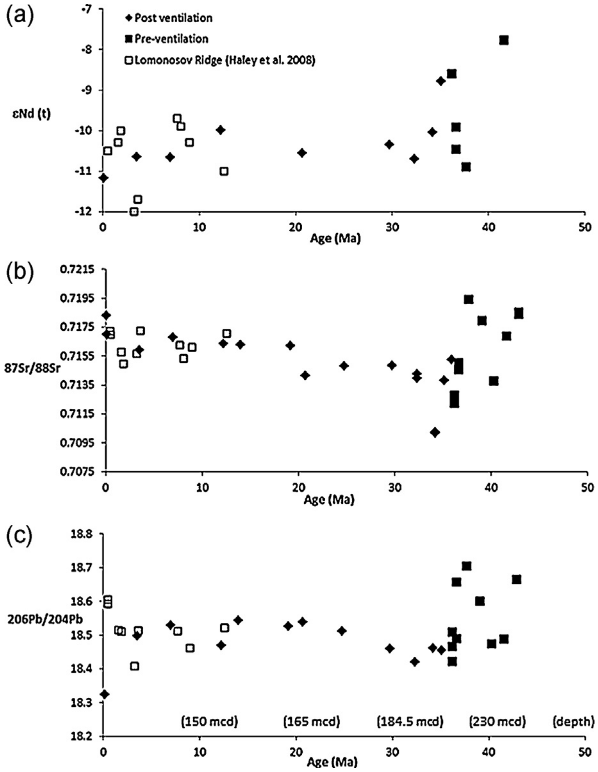

Fig. 3. Plots of ε_{Nd} (a), $^{87}Sr/^{86}Sr$ (b) and $^{206}Pb/^{204}Pb$ (c) isotope compositions of the ACEX sediments. Note that the x-axis reflects sediment age in order to accommodate the data from Haley et al. (2008). See text for details.

The Nd isotope compositions of the sediments show limited variation between −8 and −11.7, although there is a gradual shift in ε_{Nd} values from a high of −7.7 at ca 50 Ma to a low of −12 at the top of the core (Fig. 3). Higher density sampling in the period covering the zebra muds indicates that sediment sources varied rapidly during this interval. The majority of the $^{147}Sm/^{144}Nd$ ratios cluster between 0.11 and 0.12 and compare well with those for average shales and sediments (Goldstein et al., 1984), indicating that the sediments were for the most part well mixed.

The lead isotopes are corrected for in-situ decay using the U and Th concentrations measured in the core. The lead isotope ratios at the top of the core are highly variable (both age-corrected and uncorrected ratios) and reflect the infiltration of anthropogenic lead into the upper layers of the sediment through natural and biological activity (Table 1). Below the zone of anthropogenic influence (ca 51 cmd), the correlation with the Sr and Nd isotope systems is more evident (Fig. 4). The lead isotope ratios in the Arctic lake phase are variable with a tendency to have higher values that the zebra muds and Arctic Ocean phase. More detailed sampling of the ventilation phase shows a decrease in lead isotope ratios in the zebra muds (with some fluctuation) followed by a slow increase of the lead isotope compositions into the Arctic Ocean phase (Fig. 3).

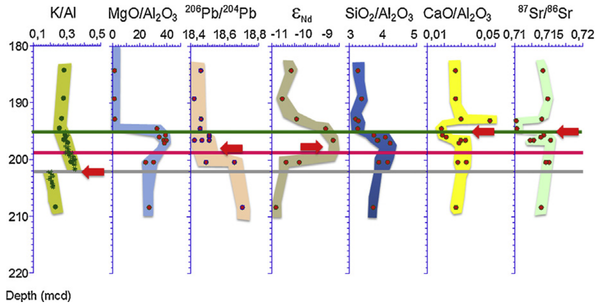

Fig. 4. (Color online.) Geochemical and isotopic excursions in the ACEX sediment core. The three horizontal lines reflect changes in sediment compositions that correlate with the depositional intervals of März et al. (2011) and the red arrows reflect three possible distinct sedimentary sources/events. The small crosses in the K/Al plot that overlap with our data are the analyses from März et al. (2011) and demonstrate that both data groups are in agreement.

4. Discussion

Changes in the chemistry and source of the sediments from the Lomonosov Ridge have been the subject of a number of studies (Haley et al., 2008; Hillaire-Marcel et al., 2013; März et al., 2011; Poirier and Hillaire-Marcel, 2009, 2011). The change in the Arctic basin from a restricted anoxic basin to an open ventilated ocean basin is reflected in the nature of the sediments (Backman et al., 2006, 2008), the fauna and flora identified in the core (Brinkhuis et al., 2006; Moran et al., 2006; Onodera et al., 2008; Stickley et al., 2008) and in the geochemistry of redox-sensitive elements and isotope systems. Poirier and Hillaire-Marcel (2009, 2011) showed that the redox-sensitive Re was concentrated in the anoxic basin and decreased after the ventilation event at 36 Ma, with their discreet data points closely matching those of the continuous measurements of März et al. (2011) within the transition zone. Similarly the initial Os isotope ratios, at first very radiogenic in the lake/epicontinental sea zone, decreased to global ocean values after ventilation due to the injection of non-radiogenic marine Os to the sedimentary load (Poirier and Hillaire-Marcel, 2009, 2011). Figs. 2 and 4 show how the concentrations of selected redox-sensitive elements such as Th, U, and Ce, and detrital-sensitive elements (K/Al) change from pre to post-ventilation and that they are consistent with the findings of März et al. (2011). Although our sampling density over 220 mcd (50 Ma) is less than the sampling density of März et al. (2011) over 12 mcd, our findings are broadly similar in that:

- redox-sensitive elements show sharp changes in concentrations across the ventilation event;
- the concentrations of the redox-sensitive elements are more variable in the anoxic basin compared to the open ocean stage;
- elements such as K and Al that are largely controlled by detrital minerals also fluctuate more widely in the anoxic basin stage and become more constant in the open ocean stage.

The geochemical fluctuations in the anoxic basin stage of the Arctic basin suggest that the basin was not entirely

Table 1
Sr, Nd and Pb isotope data for ACEX composite sediment core.

Sample 302-2A-	Depth (mcd)	Age model 2[a] (Ma)	$^{87}Sr/^{86}Sr$ residue	2 s error	Nd ppm	Sm ppm	$^{147}Sm/^{144}Nd$ residue	$^{143}Nd/^{144}Nd$ residue	2 σ error	ε_{Nd} (0)	ε_{Nd} (t)	T_{DM}	Pb[b] ppm	U[b] ppm	Th[b] ppm	$^{238}U/^{204}Pb$[c] mu	$^{232}Th/^{204}Pb$[c] kappa	$^{206}Pb/^{204}Pb$ measured ratios	$^{207}Pb/^{204}Pb$	$^{208}Pb/^{204}Pb$	$^{206}Pb/^{204}Pb$ corrected ratios[d]	$^{207}Pb/^{204}Pb$	$^{208}Pb/^{204}Pb$	$^{208}Pb/^{206}Pb$
302-2a-1X-1W-2-3cm	1.25	0.09											492	2.2	10.2	0.3	1.3	18.871	15.671	38.405	18.871	15.671	38.405	2.035
1X 1W 12-13 cm	1.35	0.09	0.71831	0.00001	23.4	4.20	0.1086	0.512065	0.000010	-11.2	-11.2	1.6	23.34	2.1	9.8	5.6	26.7	18.755	15.608	38.649	18.755	15.608	38.649	2.061
1X 1W 22-23cm	1.45	0.10																18.243	15.558	38.162	18.243	15.558	38.162	2.092
1X 1W 32-33cm	1.55	0.11	0.71697	0.00001														18.438	15.579	38.403	18.438	15.579	38.403	2.083
1X 1W 42-43cm	1.65	0.11																18.536	15.577	38.523	18.536	15.577	38.523	2.078
1X 1W 62-63cm	1.85	0.13	0.71701	0.00001														18.532	15.583	38.631	18.532	15.583	38.631	2.085
1X 1W 92-93cm	2.15	0.15																18.324	15.572	38.288	18.324	15.572	38.288	2.089
11X 2W 75-76 cm	50.69	3.5	0.71592	0.00001	26.6	4.79	0.1088	0.512090	0.000010	-10.7	-10.7	1.5	14.13	2.8	10.1	12.2	45.7	18.505	15.564	38.609	18.499	15.564	38.602	2.087
23X 2W 22-23 cm	101.55	7.0	0.71679	0.00002	36.6	9.06	0.1497	0.512089	0.000012	-10.7	-10.7	2.5	12.85	2.9	10.5	14.1	52.3	18.544	15.578	38.638	18.529	15.577	38.620	2.084
34X 2W 22-23 cm	150.72	12.3	0.71637	0.00002	35.7	6.84	0.1159	0.512119	0.000011	-10.1	-10.0	1.6	37.16	2.3	10.3	3.8	17.7	18.477	15.568	38.555	18.470	15.567	38.545	2.087
35X 2W 18-19cm	154.45	14.0	0.71630										14.76	2.4	10.6	10.1	45.8	18.566	15.580	38.654	18.544	15.579	38.622	2.083
37X- 2W 27-28cm	164.28	19.2	0.71620	0.00018									18.38	2.6	11.1	8.9	38.5	18.553	15.589	38.661	18.526	15.587	38.625	2.085
38X 2W 27-28cm	167.16	20.7	0.71414	0.00001	33.1	6.56	0.1196	0.512087	0.000010	-10.8	-10.6	1.7	19.72	2.5	10.4	8.0	33.8	18.565	15.590	38.761	18.539	15.589	38.726	2.089
40X 2W 27-28cm	174.85	24.8	0.71483	0.00001									23.03	2.9	12.1	7.7	33.5	18.542	15.581	38.668	18.512	15.579	38.627	2.087
42X 2W 27-28cm	184.26	29.7	0.71485	0.00002	40.7	8.20	0.1218	0.512093	0.000010	-10.6	-10.3	1.8	22.77	2.6	12.0	7.1	33.6	18.492	15.574	38.628	18.459	15.573	38.578	2.090
43X 2W 22-23 cm	189.20	32.3	0.71427	0.00001	36.6	7.08	0.1170	0.512072	0.000010	-11.0	-10.7	1.7	24.92	2.3	12.6	5.6	32.4	18.448	15.563	38.629	18.420	15.561	38.577	2.094
43X 2W 22-23 cm dup.	189.20	32.3	0.71396	0.00002																				
44X 3W 60-61 cm	189.58	32.5											21.44	8.1	13.4	23.4	39.8							
44X 1W 76-77 cm	192.75	34.2	0.71026	0.00002	36.4	6.93	0.1150	0.512105	0.000010	-10.4	-10.0	1.6	24.06	1.7	11.3	4.4	30.1	18.485	15.573	38.617	18.462	15.572	38.566	2.089
44X 1W 76-77 cm dup.	192.75	34.2	0.71017																					
44X 2W 95-96 cm	194.44	35.1	0.71380	0.00001	49.8	10.2	0.1243	0.512171	0.000010	-9.1	-8.8	1.7	29.69	8.9	16.6	18.5	35.6	18.556	15.582	38.627	18.455	15.577	38.565	2.090
44X 1W 106-107 cm	194.44	35.1											29.85	5.3	12.3	11.0	26.3							
45X 1W 3-4 cm	195.96	35.9	0.71525	0.00001									19.90	8.0	12.5	24.9	40.0							
45X 1W 57-58 cm b	196.5	36.2	0.71278	0.00002	41.1	10.7	0.1570	0.512188	0.000010	-8.8	-8.6	2.6	18.20	22.2		75.6		18.934	15.612	38.675	18.508	15.592	38.675	2.090
45X 1W 57-58 cm dup. b	196.5	36.2	0.71223	0.00001									18.20	22.2	12.0	75.6	42.3	18.892	15.599	38.618	18.466	15.579	38.543	2.087
45X 1W 57-58 cm b	196.5	36.2											18.20	22.2		75.6		18.848	15.598	38.620	18.422	15.579	38.620	2.096
45X 1W 57-58 cm b	196.5	36.2											18.20	22.2		75.6								
45X 1W 57-58 cm dup. b	196.5	36.2											19.10	21.6	13.8	70.2	46.2							
45X 1W 110-111 cm	197.03	36.2											19.24	17.6	14.1	56.6	46.7							
46X 2W 131-132 cm	199.81	36.6	0.71503	0.00002	20.7	3.89	0.1137	0.512081	0.000009	-10.9	-10.5	1.6												
46X 2W 131-132 cm dup.	199.81	36.6											24.11	9.9	9.1	25.4	24.0	18.802	15.597	38.694	18.657	15.591	38.651	2.072
46X 2W 132-133 cm	199.82	36.6	0.71455	0.00001	14.9	2.91	0.1181	0.512111	0.000008	-10.3	-9.9	1.7	22.24	25.7	10.3	71.6	29.6	18.898	15.597	38.607	18.490	15.578	38.554	2.085
48X 2W 21-22 cm	208.41	37.7	0.71942	0.00001	16.2	2.99	0.1117	0.51206	0.00005	-11.3	-10.9	1.6	24.58	7.8	9.1	19.7	23.7	18.820	15.604	38.735	18.705	15.598	38.690	2.068
51X 2W 6-7 cm	220.00	39.1	0.71793	0.00003									13.46	5.4	6.8	24.8	32.1	18.752	15.582	38.644	18.601	15.575	38.582	2.074
51X 2W 6-7 cm	220.00	39.1																						
54X 1W 22-23 cm	230.22	40.3	0.71377	0.00009									6.42	6.7	3.0	64.5	29.9	18.878	15.597	38.685	18.474	15.579	38.625	2.091
56X 2W 95-96 cm	241.18	41.6	0.71688	0.00001	19.8	3.79	0.1155	0.512217	0.000007	-8.2	-7.8	1.4	7.86	11.2	5.7	88.3	46.0	19.060	15.612	38.703	18.488	15.586	38.608	2.088
56X 2W 95-96 cm dup.	241.18	41.6																						
58X 2W 60-61 cm	252.00	42.9	0.71839	0.00003									7.18	6.4	4.4	55.1	39.2	19.032	15.606	38.744	18.664	15.589	38.661	2.071
58X 2W 60-61 cm dup.	252.00	42.9	0.71853	0.00003																				

[a] Model age calculations from Poirier and Hillaire-Marcel (2009, 2011).
[b] Concentrations from Table A1.
[c] Mu and kappa ratios calculated from U, Th and Pb concentrations.
[d] Age corrected ratios calculated using above mu and kappa values and decay constants for ^{235}U, ^{238}U and ^{232}Th.

restricted, but exchanged water mass with the open ocean (März et al., 2011). A critical aspect of sediment accumulation over the Lomonosov Ridge is the prominent role of sediments deposited from sea ice and iceberg rafting. St. John (2008) showed that sea ice rafting started very early, during the Mid-Eocene, whereas iceberg dispersal may only have been a factor over the past 2.7 Ma when large ice sheets developed over surrounding land and shelves (Raymo, 1994). Thus, sedimentary supplies to the Lomonosov Ridge were likely largely controlled by ice-streaming routes of ice sheets, under full glacial conditions, and by "sea ice factories", throughout much of the history of the basin discussed in this paper.

Fig. 3 illustrates the individual isotope plots for Sr, Nd and Pb isotopes. Here again, the open ocean stage of the Arctic basin is characterized by rather stable isotope compositions whereas the transition era (zebra muds) and anoxic basin are characterized by more variable isotopic compositions to be discussed further below. The strontium and lead isotope compositions of our younger sediments agree well with those of Haley et al. (2008), although the younger Nd isotope analyses of Haley et al. (2008) show more variations than those of our study. This likely reflects the greater density of sampling by Haley et al. (2008). Overall, sediment isotope compositions are more variable in the anoxic basin phase suggesting that the variations in the sources of sediments stabilized post-ventilation except for glaciation-induced isotopic excursions (Haley et al., 2008; Hillaire-Marcel et al., 2013). The anoxic basin tends to have slightly more radiogenic Sr and Pb isotope compositions compared to the open ocean phase. The average pre-ventilation isotope ratios for $^{87}Sr/^{86}Sr$ and $^{206}Pb/^{204}Pb$ are 0.7195 and 18.547, respectively, compared to 0.71502 and 18.485 after ventilation. This may reflect a larger contribution by older sources during the restricted basin phase. The radiogenic nature of the lone Nd analysis at 41.6 Ma appears to argue against an older source, but the strong overall correlation between the Nd and Sr isotopes compositions (Fig. 5a) suggests that the Nd isotope composition at 46 Ma is likely an artefact of one of several isotopic excursions in the restricted basin phase. These isotopic excursions were likely produced by periodic water mass exchange with the open ocean (März et al., 2011).

Fig. 4 shows examples of these excursions and demonstrates that:

- our K/Al ratios are concordant with those of März et al. (2011);
- our geochemical and isotopic excursions across the transition interval suggest sporadic sediment supplies from distinct sources and, at least, three distinct sedimentary events (red arrows) that correlate with the depositional intervals of März et al. (2011).

The red arrows indicate changes in sediment sources. For example the opening of Fram Strait may have led to the addition of Pan-African-derived material from the Svalbard-East Greenland passage. Furthermore, the high ε_{Nd} excursion marking the second sedimentary pulse of this transition might indicate supplies from younger material such as Tertiary basalts from Svalbard and possibly ridge basalts.

The sources of sediments to the Arctic basin are further investigated with the help of the Sr–Nd and Pb–Pb isotope plots on Fig. 5. Note the strong overlap in the Nd and Sr isotope compositions of the pre- and post-ventilation sediments (Fig. 5a), illustrating the continuity of sediment sources throughout the history of the Arctic basin. Also plotted for comparison are the isotope compositions for the Eocene to Holocene sediments of the Lomonosov Ridge (Haley et al., 2008; Hillaire-Marcel et al., 2013) and Holocene sediments from the Alpha Ridge (Winter et al., 1997). The strong overlap in the isotopic compositions of all these sediments indicates that although the relative proportions of the contributing sources may have varied over the past 50 Ma, the ultimate sources have remained largely unchanged. The isotopic composition of the older end member is represented by the Sr and Nd isotope composition of sediments from the Canadian Shelf/Mackenzie River which was ultimately largely shed from a Precambrian Shield (Hillaire-Marcel et al., 2013).

Fig. 5b shows a plot of the age-corrected lead isotope compositions from the ACEX sedimentary record. The lead isotope compositions of Miocene to Holocene sediments from the Lomonosov Ridge (Haley et al., 2008), surface sediments from the Alpha Ridge (Winter et al., 1997), core sediments from Fram Strait (Maccali et al., 2012) and the compositions of sediments from the Mackenzie and Lena Rivers (Millot et al., 2004) are plotted for comparison. Also included are the data fields for Arctic sediments from Gartside (1996) and Pan-African crust (Fagel et al., 2002). The lead isotope compositions of the Lomonosov sediments from this study overlap the Lomonosov sediment isotope compositions from Haley et al. (2008) and the most radiogenic pre-ventilation sediments from this study overlap those deposited in Fram Strait (Maccali et al., 2012). These latter sediments align with those from the Alpha Ridge (Winter et al., 1997), Arctic sediments (Gartside, 1996) and the Lomonsov Ridge (Haley et al., 2008) to form a trend that is identical to Trend A of Maccali et al. (2012). Also shown on Fig. 5b is a second trend (Trend B) that is defined by the near surface sediments in Fram Strait (Maccali et al., 2012). The Lomonosov Ridge post-ventilation sediments and least radiogenic pre-ventilation sediments from this study plot between these two trends. The shared trend (Trend A) of sediments from different parts of the Arctic basin indicates that the ultimate sources of the sediments for the Lomonosov and Alpha Ridge regions of the Arctic basin remained largely unchanged for the past 40–50 million years. Note that the lead isotope compositions of sediments from the Lena and Mackenzie rivers (Millot et al., 2004) plot at opposite ends of the Arctic sediment lead isotope trend, suggesting that these isotope compositions may represent the more extreme end-members of the sediments that are supplied to the Arctic basin. Maccali et al. (2012) interpreted Trend B to reflect the contribution of younger crustal material from Pan-African crustal terrains in Greenland whereas the low $^{206}Pb/^{204}Pb$ end of Trend A reflects the addition of contribution of younger Eurasian sources such as the Laptev Sea and Lena River (Millot et al., 2004; Tütken et al., 2002) as well as small possible

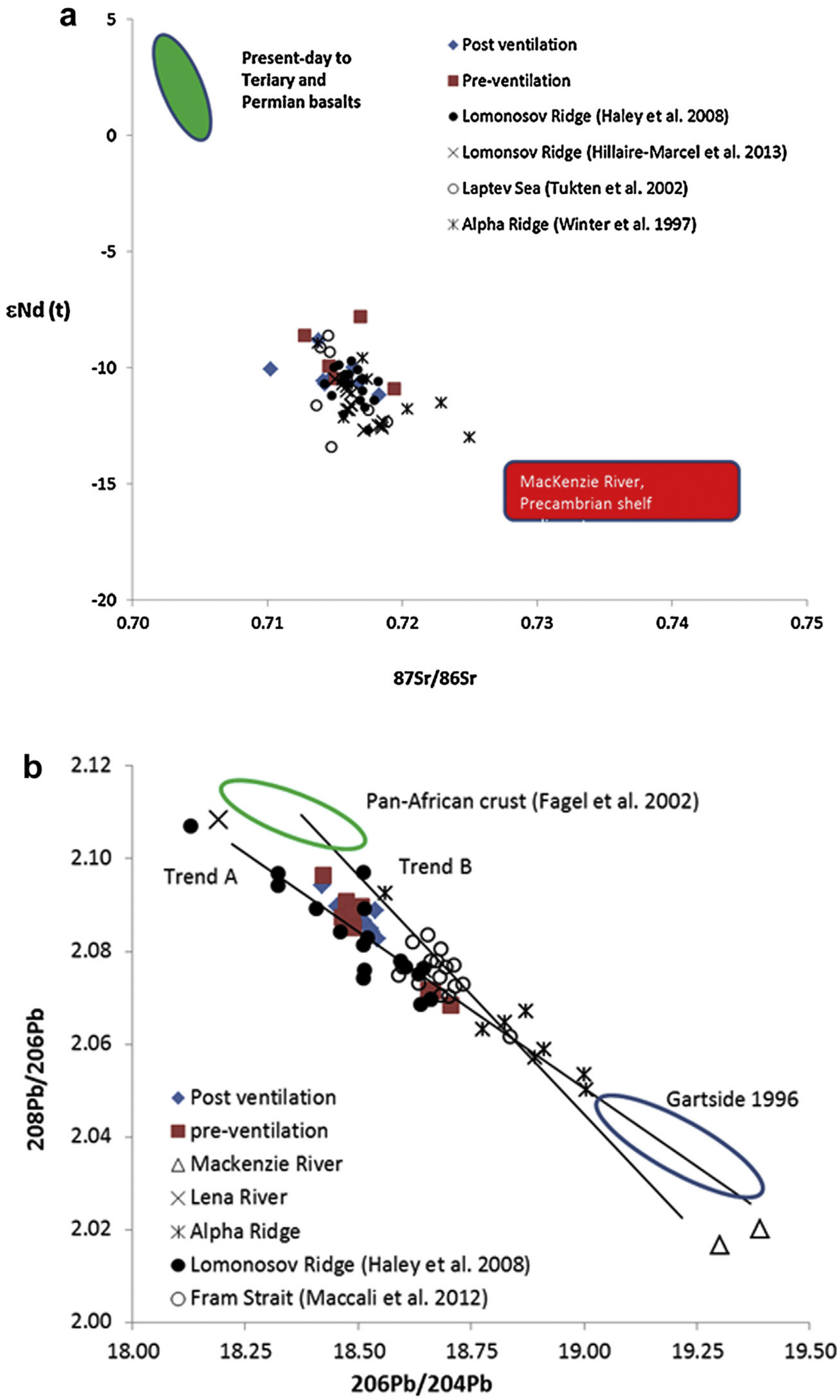

Fig. 5. (Color online.) a: plot of the ε_{Nd} values versus the $^{87}Sr/^{86}Sr$ isotope ratios of the ACEX sediments. There is a general overlap of the isotope data from sediments from various Arctic locations. Overall, the Nd and Sr isotope data suggest a mixture of older Precambrian-sourced sediments from the Canadian Shelf and younger sediments from Eurasian sources possibly including present-day to Tertiary and Permian basalts. See text for details; b: plot of the $^{208}Pb/^{204}Pb$ isotope versus $^{206}Pb/^{204}Pb$ isotope compositions of the ACEX sediments with comparison to the lead isotope compositions of sediments from other Arctic Ocean localities and from Fram Strait. Mackenzie, Red and Lena Rivers from Millot et al. (2004). Alpha Ridge data from Winter et al. (1997). The A and B trends reproduce those of Maccali et al. (2012) indicating that before ventilation, sediments to the Arctic basin were dominated by older sources, whereas younger sources were introduced following ventilation. See text for details.

contributions from present-day to Permian basaltic rocks in and around the Arctic basin. The Mackenzie and Red Rivers represents the supply of sediments shed from the Canadian Precambrian Shield that ultimately comprise much of the Canadian shelf. The predominance of higher $^{206}Pb/^{204}Pb$ isotope ratios prior to the ventilation event suggests that Canadian shelf sources dominated during the anoxic basin era (Fig. 3c).

The Sr–Nd–Pb isotope plots of Fig. 5 suggest that sediments in the Arctic basin were derived from three major sources: one end member of the Arctic basin sediment mixture is controlled by the supply of sediments from the erosion of Precambrian terrains such as the Northwest Canadian Shield whereas the other two end-members are controlled by the erosion of younger Pan-African (Caledonian) or Eurasian crust (Laptev Sea and Lena River). This latter component could also contain sediments derived from the erosion of Phanerozoic to present-day basaltic crust (Permian Siberian Trapps, Tertiary Basalts and present-day mid-ocean ridge basalts: MORB). The slight predominance of radiogenic strontium and lead isotope ratios in the restricted anoxic basin stage provides evidence that sediments sourced from the Canadian Shield were predominant over the Eurasian sediment sources, although the Nd isotope compositions show no substantial difference between the pre- and post-ventilation eras (Fig. 5a). The decrease in the strontium and lead isotope compositions following the ventilation event indicates that open ocean circulation favoured a greater contribution from Eurasian sources and/or Pan-African sources. The variable Sr–Nd–Pb isotopic compositions identified in the pre-ventilation era reflect the waxing and waning of these two sources during periodic water mass exchanges with the open ocean as suggested by März et al. (2011) on the basis of the elemental geochemistry of the sediments.

Thus, the restricted basin phase of the Arctic basin appears to have favoured a greater contribution of older sediments (source #1; Fig. 1) on the Lomonosov Ridge whereas following ventilation, the establishment of stable sediment sources with a greater contribution from younger sources suggests that the passage of water through Fram Strait enhanced and stabilized erosion of the Eurasian shelf (sources #2 and possibly #3; Fig. 1). This is supported by the presence of two diverging trends (A and B) on Fig. 5b. This shared sediment source trends between sediments of the Lomonosov ridge and Fram Strait (Carignan et al., 2008; Maccali et al., 2012) underlines the importance of the flow of water through Fram strait in controlling and stabilizing the flow of water in the Arctic Ocean and ultimately the source of sediments deposited along the Lomonosov Ridge.

5. Conclusions

Geochemical and isotopic analyses of sediments from the composite ACEX sediment core obtained from the Lomonosov ridge in the Arctic Ocean provide constraints for the evolution of the Arctic basin from restricted anoxic basin to open ventilated ocean. The geochemical data illustrate:

- the depletion and concentration of redox-sensitive elements in the Eocene anoxic Arctic basin;
- the ventilation of the restricted basin and formation of the modern Arctic Ocean is reflected in the stabilization of both redox-sensitive elements and elements controlled by detrital minerals (this study, März et al., 2011; Poirier and Hillaire-Marcel, 2009, 2011).

The Sr, Nd and Pb isotope compositions of the sediments are also more variable in the pre-ventilation era compared to the post-ventilation era suggesting either the establishment of the open ocean stabilized sediment sources, and/or that enhanced supplies from sea ice factories became more important in response to the Cenozoic large-scale cooling trend (e.g., St. John, 2008). Nevertheless, the variability in the isotopic compositions during the restricted basin phase supports the notion that the basin might have experienced periodic injections of water from the open ocean (März et al., 2011). Although the isotopic data indicate that sediment sources were broadly constant throughout the history of the Arctic basin, strontium and lead isotope compositions suggest that older crustal sources attributed to sediments shed from the Canadian Shield dominated during the restricted basin phase. Younger crustal contributions increased following ventilation of the basin and the establishment of the modern Arctic Ocean. The similarity in isotopic compositions and sediment sources for sediments from the Lomonosov ridge and Fram Strait (Maccali et al., 2012, 2013) underscore the importance for the passage of water through Fram Strait for controlling both the circulation and sediment deposition within the Arctic Ocean and the importance the contribution of water masses to the North Atlantic Ocean.

Acknowledgements

This article is dedicated to Jean Carignan: protégé, peer, mentor and friend. This study was supported by NSERC grants to RS and CHM.

Appendix A. Supplementary material

Supplementary material associated with this article can be found in the online version available at http://dx.doi.org/10.1016/j.crte.2015.02.008.

References

Backman, J., Moran, K., McInroy, D.B., Mayer, L.A., Expedition 302 Scientists, 2006. Arctic Coring Expedition (ACEX). Proc. IODP 302, 302, http://dx.doi.org/10.2204/iodp. proc.302.101.2006.

Backman, J., Jakobsson, M., Frank, M., Sangiorgi, F., Brinkhuis, H., Stickley, C., O'Regan, M., Løvlie, R., Pälike, H., Spofforth, D., Gattacecca, J., Moran, K., King, J., Heil, C., 2008. Age model and core-seismic integration for the Cenozoic Arctic Coring Expedition sediments from the Lomonosov Ridge. Paleoceanography 23, PA1S03, http://dx.doi.org/10.1029/2007PA001476.2008.

Belshaw, N.S., Freedman, P.A., O'Nions, R.K., Frank, M., Guo, Y., 1998. A new variable dispersion double-focussing plasma mass spectrometer with performance illustrated for Pb isotopes. Int. J. Mass Spectrom. 181, 51–58.

Brinkhuis, H., et al., 2006. Episodic fresh surface waters in the Eocene Arctic Ocean. Nature 441, 606–609.

Carignan, J., Hillaire-Marcel, C., De Vernal, A., 2008. Arctic vs. North Atlantic water mass exchanges in Fram Strait from Pb isotopes in sediments. Can. J. Earth Sci. 45, 1253–1263.

Fagel, N., Innocent, C., Gariepy, C., Hillaire-Marcel, C., 2002. Sources of Labrador Sea sediments since the Last Glacial Maximum inferred from Nd-Pb isotopes. Geochim. Cosmochim. Acta. 66, 2569–2581.

Gartside, M., 1996. Sources et inventaire du plomb anthropique dans les sédiments de l'Océan Arctique profond (M. S. Thesis). Université Québec à Montréal, Montréal, Canada (79 p.).

Goldstein, S.L., O'Nions, R.K., Hamilton, P.J., 1984. A Sm-Nd isotopic study of atmospheric dusts and particulates from major river systems. Earth Planet. Sci. Lett. 70, 221–236.
Gutjahr, M., Frank, M., Stirling, C.H., Klemm, V., van de Flierdt, T., Halliday, A.N., 2007. Reliable extraction of a deepwater trace metal isotope signal from Fe-Mn oxyhydroxide coatings of marine sediments. Chem. Geol. 242, 351–370.
Haley, B.A., Frank, M., Spielhagen, R.F., Fietzke, J., 2008. Radiogenic isotope record of Arctic Ocean circulation and weathering inputs of the past 15 million years. Paleoceanography 23, PA1S13, http://dx.doi.org/10.1029/2007PA001486.
Hillaire-Marcel, C., Maccali, J., Not, C., Poirier, A., 2013. Geochemical and isotopic tracers of Arctic sea ice sources and export with special attention to the Younger Dryas interval. Quat. Sci. Rev. 79, 184–190.
Maccali, J., Hillaire-Marcel, C., Carignan, J., Reisberg, L.C., 2012. Pb isotopes and geochemical monitoring or Arctic sedimentary supplies and water mass export through Fram Strait since the Last Glacial Maximum. Paleoceanography 27, PA1201, http://dx.doi.org/10.1029/2011PA002152.
Maccali, J., Hillaire-Marcel, C., Carignan, J., Reisberg, L.C., 2013. Geochemical signatures of sediments documenting Arctic sea ice and water mass export through Fram Strait since the Last Glacial Maximum. Quat. Sci. Rev. 64, 136–151.
März, C., Schnetger, B., Brumsack, H.-J., 2011. Paleoenvironmental implications of Cenozoic sediments from the central Arctic Ocean (IODP Expedition 302) using inorganic geochemistry. Paleoceanography 25, PA3206, http://dx.doi.org/10.1029/2009PA001860.
Millot, R., Allègre, C.J., Gaillardet, J., Roy, S., 2004. Lead isotopic systematics of major river sediments: a new estimate of the Pb isotopic composition of the Upper Continental Crust. Chem. Geol. 203, 75–90.
Moran, K., et al., 2006. The Cenozoic palaeoenvironment of the Arctic Ocean. Nature 441, 601–605.
Onodera, J., Takahashi, K., Jordan, R.W., 2008. Eocene silicoflagellate and ebridian paleoceanography in the central Arctic Ocean. Paleoceanography 23, PA1S15, http://dx.doi.org/10.1029/2007PA001474.
Pagani, M., Pedentchouk, N., Huber, M., Sluijs, A., Schouten, S., Brinkhuis, H., Sinninghe Damsté, J.S., Dickens, G.R., Expedition-Scientists, 2006. Arctic hydrology during global warming at the Palaeocene-Eocene thermal maximum. Nature 442, 671–675.
Poirier, A., Hillaire-Marcel, C., 2009. Os isotope insights into major environmental changes of the Arctic Ocean during the Cenozoic. Geophys. Res. Lett. 36, L11602, http://dx.doi.org/10.1029/2009GL037422.
Poirier, A., Hillaire-Marcel, C., 2011. Improved Os isotope stratigraphy of the Arctic Ocean. Geophys. Res. Lett 38, L14607, http://dx.doi.org/10.1029/2011GL047953.
Raymo, M.E., 1994. The initiation of Northern Hemisphere glaciation. Annu. Rev. Earth Planet. Sci. 22, 353–383.
Sluijs, A., et al., 2006. Subtropical Arctic Ocean temperatures during the Paleocene/Eocene thermal maximum. Nature 441, 610–613.
Sluijs, A., Röhl, U., Schouten, S., Brumsack, H.-J., Sangiorgi, F., Sinninghe Damsté, J.S., Brinkhuis, H., 2008. Arctic late Paleocene–Early Eocene paleoenvironments with special emphasis on the Paleocene-Eocene thermal maximum (Lomonosov Ridge Integrated Ocean Drilling Program Expedition 302). Paleoceanography 23, PA1S11, http://dx.doi.org/10.1029/2007PA001495.
Stickley, C.E., Koc, N., Brumsack, H.-J., Jordan, R.W., Suto, I., 2008. A siliceous microfossil view of Middle Eocene Arctic paleoenvironments: a window of biosilica production and preservation. Paleoceanography 23, PA1S14, http://dx.doi.org/10.1029/2007PA001485.
St. John, K., 2008. Cenozoic ice rafting history of the central Arctic Ocean: Terrigenous sands on the Lomonosov Ridge. Paleoceanography 23, PA1S05, http://dx.doi.org/10.1029/2007PA001483.
Tanaka, T., Togashi, S., Kamioka, H., Amakawa, H., Kagami, H., Hamamoto, T., Yuhara, M., Orihashi, Y., Yoneda, S., Shimizu, H., Kunimaru, T., Takahashi, K., Yanagi, T., Nakano, T., Fujimaki, H., Shinjo, R., Asahara, Y., Tanimizu, M., Dragusanu, C., 2000. JNdi-1: a neodymium isotopic reference in consistency with LaJolla neodymium. Chem. Geol. 168, 279–281.
Tütken, T., Eisenhauer, A., Wiegand, B., Hansen, B.T., 2002. Glacial-interglacial cycles in Sr and Nd isotopic composition of Arctic marine sediments triggered by the Svalbard/Barents Sea ice sheet. Mar. Geol. 182, 351–372.
Winter, B.L., Johnson, C.M., Clark, D.L., 1997. Strontium, neodymium, and lead isotope variations of authigenic and silicate sediment components from the Late Cenozoic Arctic Ocean: implications for sediment provenance and the source of trace metals in seawater. Geochim. Cosmochim. Acta 61, 4181–4200.